JOURNAL OF SOLID STATE CHEMISTRY 81, 40–50 (1989)

Electron Microscopic Study on the Layered Structure Substituted for Cation Sites in $BaMnO_3$

H. SHIBAHARA

Department of Chemistry, Kyoto University of Education, Fushimi-ku, Kyoto 612, Japan

Received September 19, 1988; in revised form March 13, 1989

Structures of new phases represented by the formula $Ba_{1-x}Me_xMnO_3$ (Me = metal ion) were studied by high-resolution electron microscopy. $Ba_{1-x}Me_xMnO_3$ was formed by substituting Me cations (Me = Sr and Ca ions) for cation sites in $BaMnO_3$. Electron microscope images showed that cation substitution for Ba ions in the $BaMnO_3$ system induced a phase transformation for a 2H phase into other phases with a longer periodicity than that of 2H. The structure images showed that the structure of the two-layer phase was transformed into a modified structure accompanying a shear normal to the c-axis in hexagonal lattice. The present results support the mechanism which was previously suggested by the present author and his colleague in the case of the phase transformation of the $BaMn_{1-x}M_xO_{3-x}$ system (M = Ta and Zn ions) and the production of oxygen-defective structure of $BaMnO_{3-x}$ due to beam irradiation.

Introduction

The perovskites with the general formula XYO_3 have been extensively studied because of their interesting ferroelectric and magnetic properties. The structural modifications in the oxides of XYO_3 were studied by several authors by means of X-ray diffraction with the aid of finding some correlation between the nature of the substituent elements and a crystal structure (*1–4*). When ions of more than one element are present in the X or Y position, the possibility of these ions being ordered exists. It has been stimulated by the fact that composition change and structural variations could have profound effects upon the electrical and magnetic properties of the crystals (*5*). Detailed structural refinements of these compounds would probably be very helpful in understanding their bonding and magnetic or ferroelectric properties.

The systems of $BaMnO_{3-x}$ and $SrMnO_{3-x}$ are known to be layered structures closely related to that of perovskite with oxygen deficiency and based on a stacking of close-packed $Ba(Sr)O_3$ layers with Mn metals occupying interlayer octahedral sites (*3–6*). As far as $BaMnO_3$ is concerned, the low-temperature form at normal pressure has a 2H structure (H = hexagonal) which means a two-layer sequence of hh where h represents a hexagonal BaO_3 layer. On the other hand, the perovskite structure of XYO_3 consists of cubic close-packed XO_3 layers. Variety in structure of XO_3 originates in the mixture of cubic and hexagonal packing. The present author and his colleague suggested previously that the mechanism for the phase transformation of a 2H structure

0022-4596/89 $3.00

in $Ba^{2+}Mn^{4+}O_3$ into nonstoichiometric states was due to electron beam irradiation by *in situ* observation with an electron microscope (*7*). This proposed mechanism explained that the reduction by beam irradiation generates Mn^{3+} ions in octahedra with lower coordination number and induces their displacement to avoid the electrostatic repulsion between shorter face-sharing octahedra because of Mn^{3+} ions having a little larger ion radii than those of Mn^{4+}. In addition, previous to this study the present author reported the relation of a few phases formed by the introduction of Ta and Zn ions into $BaMnO_{3-x}$, using the electron diffraction patterns and the structure images formed by a high-resolution electron microscope (*8*). The summarized results from this report were as follows: cation substitution for Mn ions in $BaMnO_{3-x}$ system induced a phase transformation of 2H phase into other phases with a longer periodicity than that of 2H. A structure model of 2H phase in $BaMnO_3$ is shown in Fig. 1a projected along 010 direction in hexagonal unit cell. In the case of Ta ion substitutions, for example, the structure images showed that a 2H phase was transformed into a 15-layer phase with an accompanying shear normal to the *c*-axis in hexagonal unit cell. The structure model of the 15-layer phase proposed by the author in Ref. (*8*) is described in Fig. 1b. The result, which was characterized by the Mn sites located in oxygen octahedra being substituted partly by some Ta atoms, was derived on the basis of the assumption that Mn^{3+} ions induced by Ta ion substitution having the effective ion radii—ions a little larger than those of Mn^{4+}—are able to play an important role in creating a shear to avoid the electrostatic repulsion among neighboring face-sharing octahedra. Serial studies about the structural modification in $BaMn_{1-x}M_xO_{3-x}$ (M = Ta, Zn) system demonstrated that a high-resolution electron microscope observation is sensitive enough to examine the local phase with relation to the layered structure

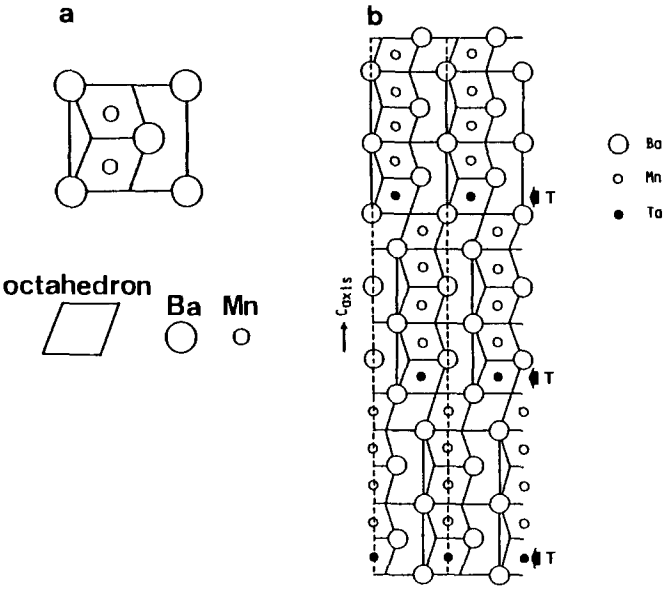

FIG. 1. (a) Structure model of $BaMnO_3$ (2H) projected along the (010) direction in the hexagonal unit cell. (b) A projected structure model containing some Ta atoms represented by dark circles with 15-layer periodicity along the *c*-axis quoted from Ref. (*8*).

in an atomic scale. And the local structure found for the samples, which were too polycrystalline for study by an X-ray diffraction method, was detectable only by electron diffraction and high-resolution imaging.

In order to examine the mechanism stated above, the present author studied the relation among a few phases formed by the introduction of Sr/Ca ions into $BaMnO_3$ by means of X-ray powder diffraction and high-resolution electron microscopy. The attention focused on direct observation by electron microscopy in an atomic scale for some layered structures. As part of a continued study to demonstrate the causes producing a layered structure with a longer periodicity than that of 2H along the c-axis in $BaMnO_{3-x}$ complexed oxide, the results with a stacking fault and layered structure formed in $BaMnO_3$ are described in this paper.

Experimental

A series of the present samples was prepared by the conventional solid-state reaction technique. The reactants used for sintering were reagent grade. First, 2H phase of barium manganate used as the starting material in this experiment was prepared by the procedure described by the author (*7, 8*). Subsequently, the products were mixed with weighed amounts of hyperpure strontium carbonate or calcium carbonate. The mixing time for preparing the mixtures was 24 hr. The mixture containing strontium carbonate or calcium carbonate was heated in O_2 at a flow rate of about 1000 ml/min in an electric furnace. The temperature was raised slowly and held at 1150°C or higher for 6–12 hr, followed by very slow cooling to room temperature. The characterization studies by the X-ray powder diffraction were all on the sintered samples. X-ray powder diffraction patterns of the samples were obtained at 25°C and recorded by using Ni-filtered Cu$K\alpha$ radiation. For electron microscope observation, the samples were finely ground and dispersed in absolute ethanol and then mounted onto holey carbon microgrids. High-resolution electron microscope images were taken with a JEM-2000EX electron microscope. For observation in an electron microscope, a very thin fragment was selected and its orientation was adjusted so as to make the incident beam direction vertical to the c^*-axis in reciprocal space by using a goniometer stage in order to detect the difference in structure due to the stacking sequence. The samples were not subjected to change in crystal structure by normal electron beam irradiation during observation.

Experimental Results and Discussion

1. X-Ray Powder Diffraction Study

The sample used as the starting material gave an X-ray powder diffraction pattern of a 2H structure with lattice parameters of $a = 0.57$ nm, $c = 0.48$ nm, which also agreed well with that of the previously published studies (*5, 6*). All of the lines belonged to the hexagonal type of the pattern of $BaMnO_3$ as shown in Fig. 2a, which was the same one as that previously reported by the present author (*8*). Subsequently, the samples in which some metal ions were substituted were also verified with an X-ray powder diffraction method. All the sintered products were black. Figs. 2b and 2c show the X-ray powder diffraction patterns of the samples mixed with $CaCO_3$ and $SrCO_3$ of 0.1 mole ratio to $BaMnO_3$. For the sake of comparing them, they were indexed on the basis of the two-layer hexagonal unit cell. Though their predominant phases were $BaMnO_3$ (2H), the diffraction lines corresponding to (101) and (110) of 2H structure in $BaMnO_3$ were shifted slightly to high Bragg angles when compared with those of Fig. 2a. And, especially 101 lines had a

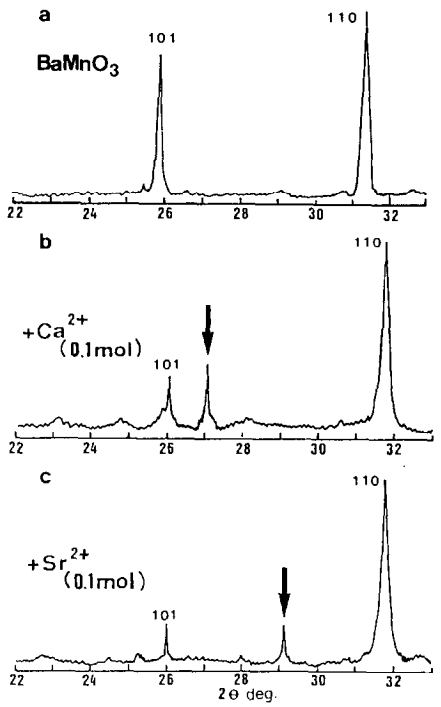

FIG. 2. X-ray powder diffraction patterns of (a) a two-layer phase used as starting material in which indices are based on a two-layer hexagonal lattice, (b) the samples mixed with $CaCO_3$, and (c) $SrCO_3$ of about 0.1 in mole ratio to $BaMnO_3$.

decreasing tendency in their intensities. The c-axis of the hexagonal unit cell is perpendicular to the close-packed layers and is in the 111 direction of the perovskite pseudocubic cells. These results indicate that the samples have a tendency toward ordering of BaO_3 layers normal to the c-axis in the hexagonal unit cell and reducing their lattice constants along the c-axis to about 2%. Some characteristic lines corresponding to other phases were also noted in Figs. 2b and 2c as indicated by arrows, which are similar to those of results reported previously by the present author for the samples formed by adding Ta_2O_5 or ZnO to $BaMnO_{3-x}$ (*8*). From only the X-ray powder diffraction patterns of Figs. 2b and 2c, the periodicity along the c-axis in the hexagonal lattice due to ordering of the BaO_3 subarray could not be examined in detail because of the mixtures of a few phases.

Shannon and Prewitt (*9*) reported that the effective ion radii of Ba^{2+}, Sr^{2+}, and Ca^{2+} in the octahedral site are 0.15, 0.13, and 0.12 nm, respectively. Sr^{2+} and Ca^{2+} ions have almost the same effective radii as Ba ions, and so they can substitute for Ba ions in a charge-compensating manner. A similar situation was found in the case of the substitution for the Ba-site by a small amount of Sr^{2+} or Ca^{2+} ions in barium titanate ($BaTiO_3$) which has the typical perovskite structure (*10–12*). The substitutions of X-cation with different sizes could change the effective size of the unit cell without any great structural change of the matrix while maintaining Y-cation constant in XYO_3. The present experimental condition seems to be depicted by the following chemical reaction:

$$Ba^{2+}Mn^{4+}O_3^{2-} + 2xMe^{2+}CO_3 \rightarrow (Ba^{2+}_{1-2x}Me^{2+}_{2x})MnO_3 + 2xCO_2 \uparrow + xO_2 \uparrow \quad (Me^{2+} = \text{Sr, Ca ions}).$$

The chemical reaction described above indicates that some Sr or Ca ions substitute for Ba ions by releasing gases (CO_2, O_2) under the valence compensation principle and without anionic deficiencies. Consequently, Sr^{2+} and Ca^{2+} ions having the effective ion radii a little smaller than the Ba^{2+} ions ($Sr^{2+}/Ba^{2+} = 0.87$, $Ca^{2+}/Ba^{2+} = 0.80$) are able to play an important role in creating a shear to avoid the electrostatic repulsion among neighboring XO_3 layers caused by a decrease in the size of the XO_3 layers. This situation is analogous to that of the phase modification introduced by electron beam irradiation and the substitution for Y-site with some cations in XYO_3 as reported by the present author and his colleague (*7, 8*). Therefore, the present experimental treatment could simulate the phase transformation of the 2H structure into another phase based on the mechanism mentioned above.

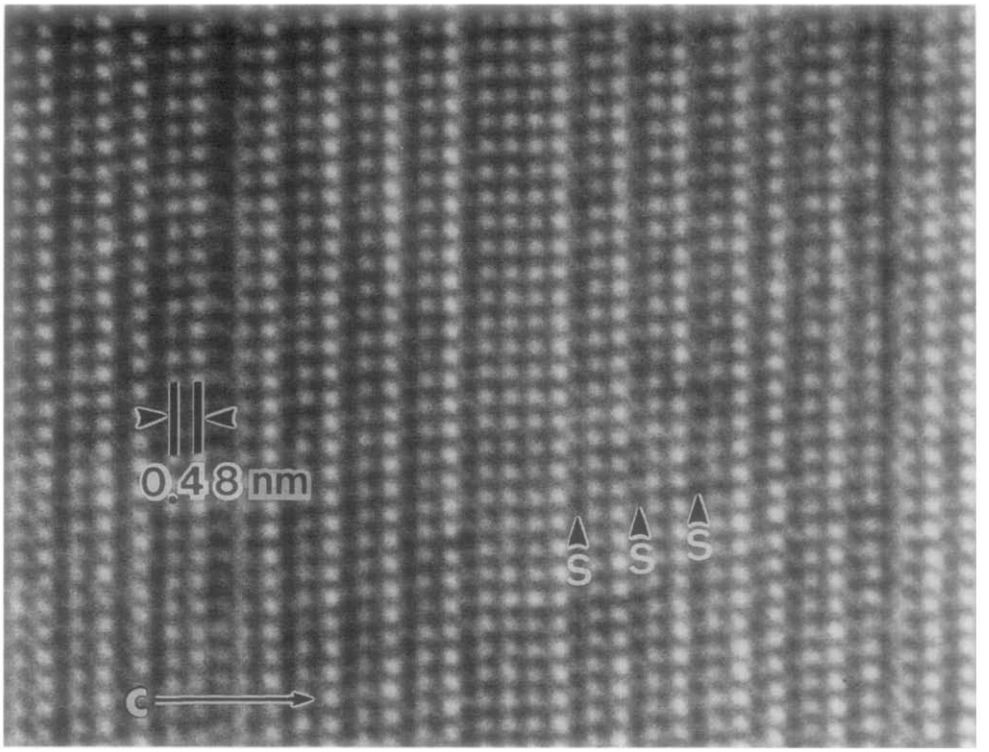

FIG. 3. High-resolution electron micrograph of the sample by sintering with $CaCO_3$. The S arrows indicate atomic displacements due to a shear structure.

2. *Electron Microscopy and Electron Diffraction Study*

2.1. Introduction of Ca ions. Figure 3 shows the electron microscope of the sample mixed with $CaCO_3$ corresponding to that of Fig. 2b. The fringes of shear structure due to disorderly stacking faults along the *c*-axis were observed in Fig. 3. From the image of Fig. 3, it could be elucidated that a shear in the BaO_3 layer with a displacement vector of $\pm\frac{1}{3}(1\bar{1}0)$ took place and produced a new periodicity in the crystal structure. The contrast in the image of Fig. 3 as indicated by the S arrows shows evidence of having a shear structure due to such an atomic displacement. By using the schematic structure model, a displacement vector of $\pm\frac{1}{3}(1\bar{1}0)$ normal to the *c*-axis in hexagonal unit cell is described in Figs. 4a and 4b, which represent the projections along the *c*- and *b*-axis of the hexagonal cell in real space, respectively. BaO_3 layers are

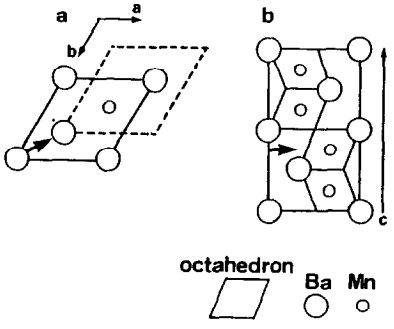

FIG. 4. Schematic structure model of $BaMnO_3$ having a shear vector of $\pm\frac{1}{3}(1\bar{1}0)$. (a) The *c*-axis projection; (b) the *b*-axis projection. The framework with the dotted lines illustrates the unit cell arrangement after displacing by a vector of $\pm\frac{1}{3}(1\bar{1}0)$.

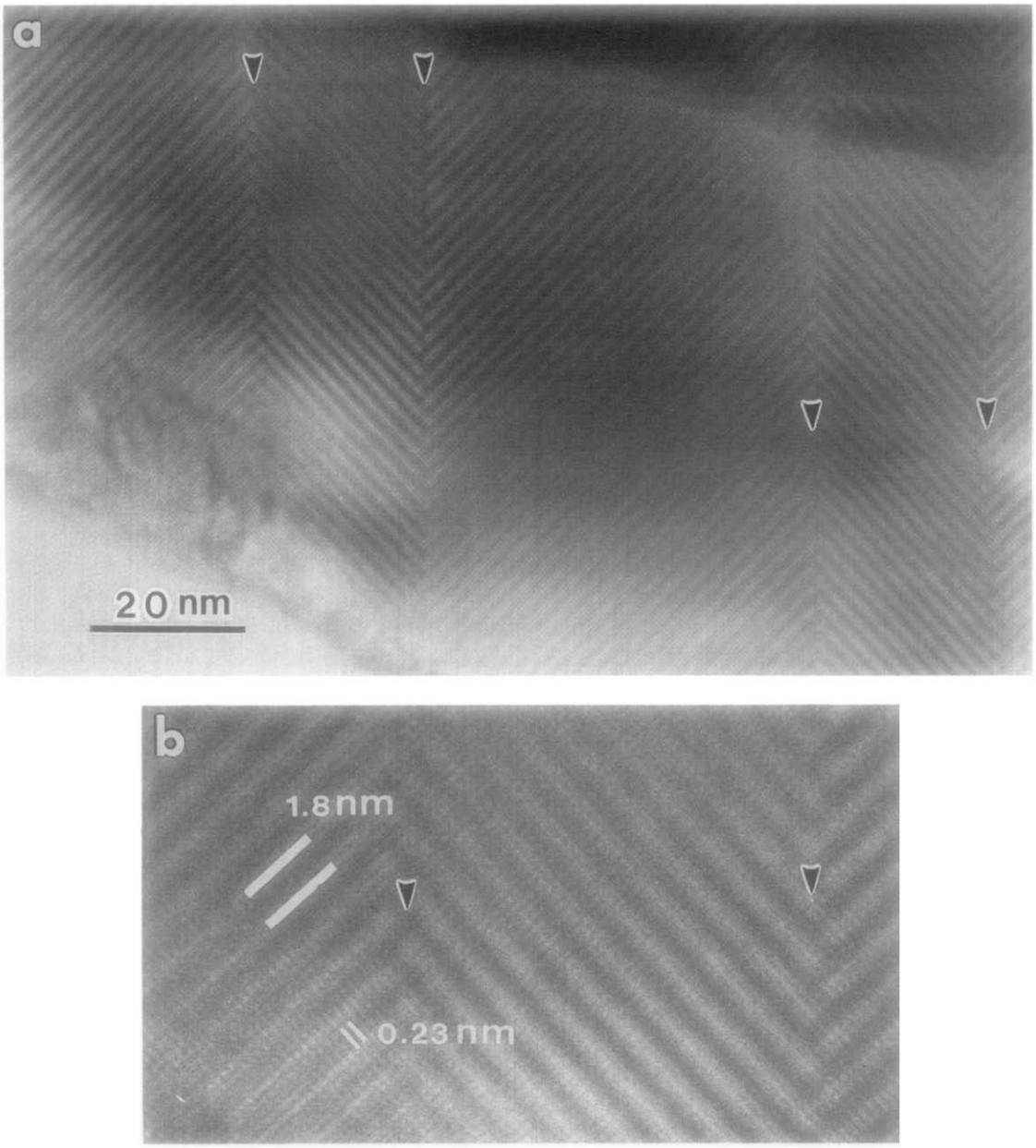

FIG. 5. Electron micrograph (a) and enlargement (b) of the twin structure observed in the sample by sintering with $CaCO_3$ to $BaMnO_3$. Twin planes as indicated by the arrows could be interpreted as being (104) planes.

arranged normal to 001 direction. Namely, a longer periodicity than that of a 2H structure could be produced by displacing some BaO_3 layers normal to the c-axis as indicated by arrows in Figs. 4a and 4b.

Figures 5a and 5b show the observed image of the twin structure for the sample mixed with $CaCO_3$ and its enlargement, respectively. The periodicity of about 1.8 nm detected in the image corresponds to the

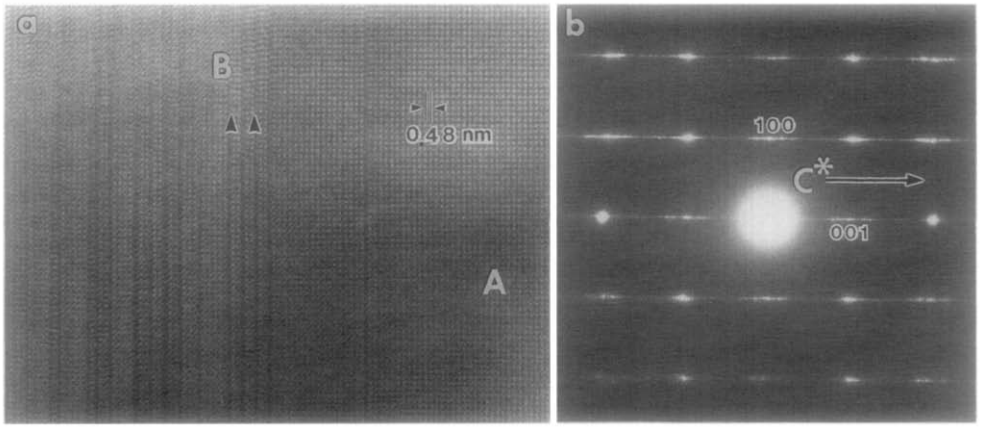

FIG. 6. Electron micrograph (a) and diffraction pattern (b) of the sample by sintering with $SrCO_3$, taken with an incident beam parallel to the (010) direction in the hexagonal unit cell.

eight times of (001) spacing in a 2H structure. If the structure with long periodicity of an eight-layer has pseudohexagonal stacking, the twin plane as indicated by the arrows in Figs. 5a and 5b could be interpreted as consisting of (104) plane.

2.2. Introduction of Sr ions. Figures 6a and 6b show the electron microscope image and electron diffraction pattern of the sample mixed with $SrCO_3$ corresponding to that of Fig. 2c, which was taken with the incident electron beam parallel to the 010 direction in the hexagonal unit cell. Similar behavior to Fig. 6a was observed for the sample substituted by Ca ions as shown in Fig. 3. Figures 7a and 7b show the enlarged images of the areas designated by A and B in Fig. 6a, respectively. By image simulation on the basis of the multi-slice method (*13, 14*) the previous report (*8*) demonstrated that the white dot array such as found in Fig. 7a represents the arrangement

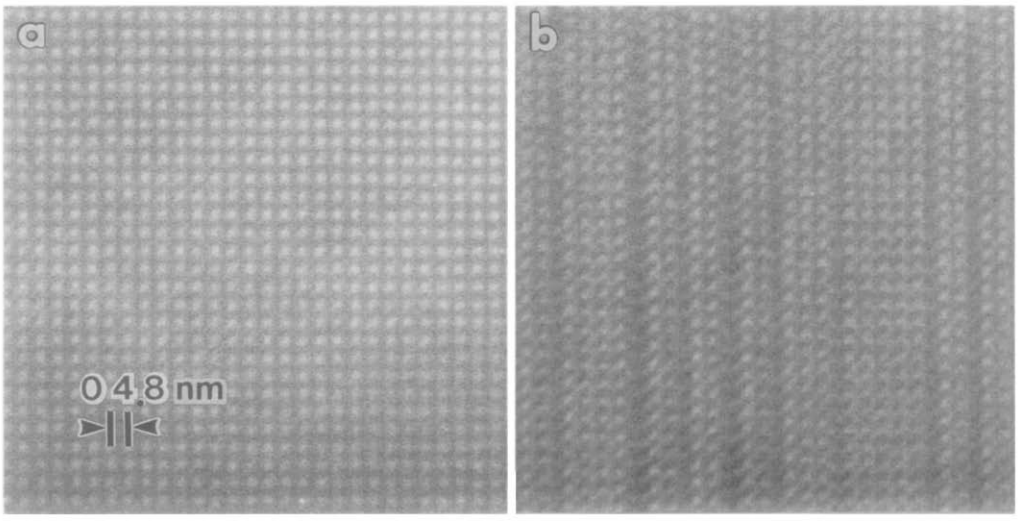

FIG. 7. Enlargements of the area marked by A and B in Fig. 6a.

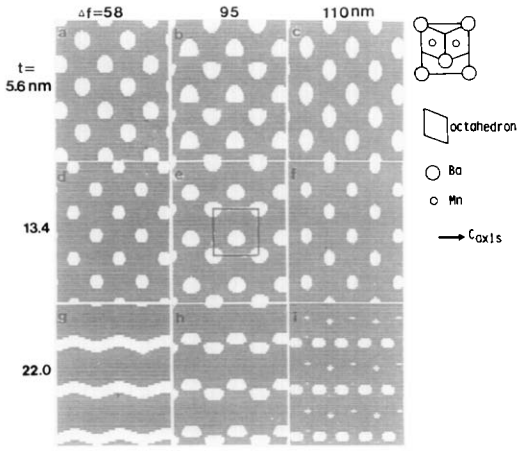

FIG. 8. Image calculation on 2H structure in $BaMnO_3$ quoted from Ref. (*8*) by the author.

of Ba toms in 2H structure of $BaMnO_3$ under the present imaging conditions of a sample thickness of about 10 nm and a defocus value of 50–100 nm in underfocus. Figure 8 shows, for reference, the result of image calculation on the 2H structure of $BaMnO_3$ assuming almost the same imaging condition as that of Fig. 7, which was quoted from the previous report by the author (*8*). The atomic positions of Ba could be estimated through the image contrast directly. Area A in Fig. 6a showing the periodicity of about 0.48 nm which corresponds to the lattice constant of 2H structure along the *c*-axis could be considered to be $BaMnO_3$ (2H) phase. But the characteristic contrast due to disorderly stacking faults normal to the *c*-axis as indicated by arrows

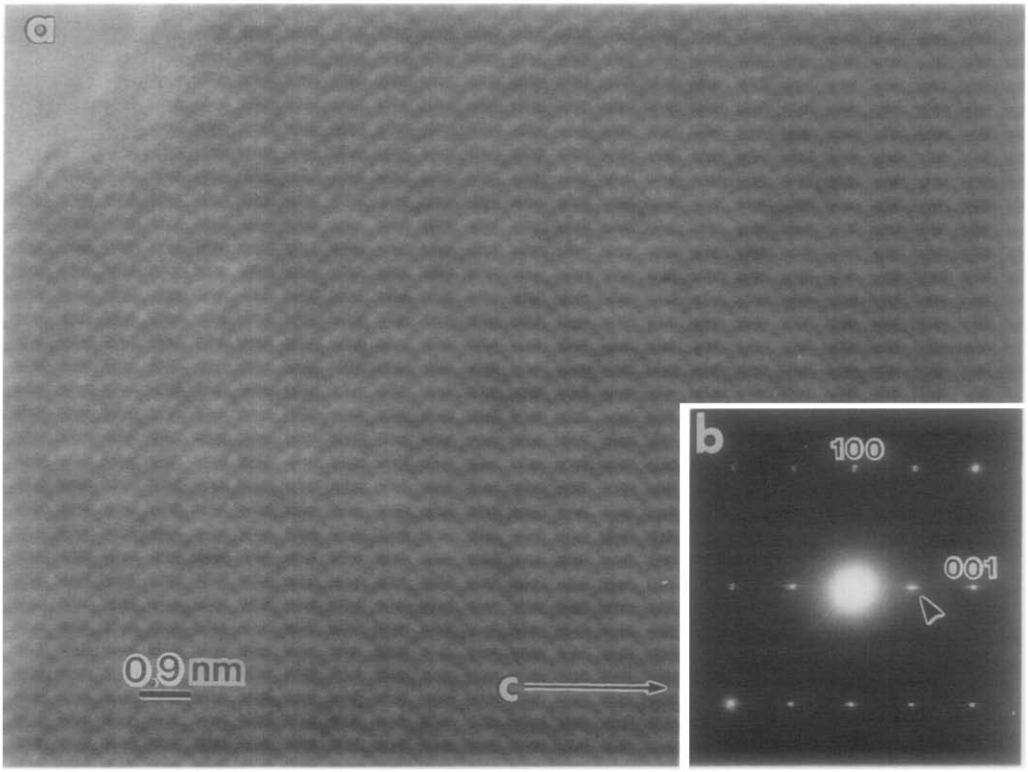

FIG. 9. High-resolution electron micrograph (a) and diffraction pattern (b) of the sample with $SrCO_3$ prepared by heating sufficiently. In (a) the periodicity of about 0.9 nm which corresponds to the four-layer structure is observed.

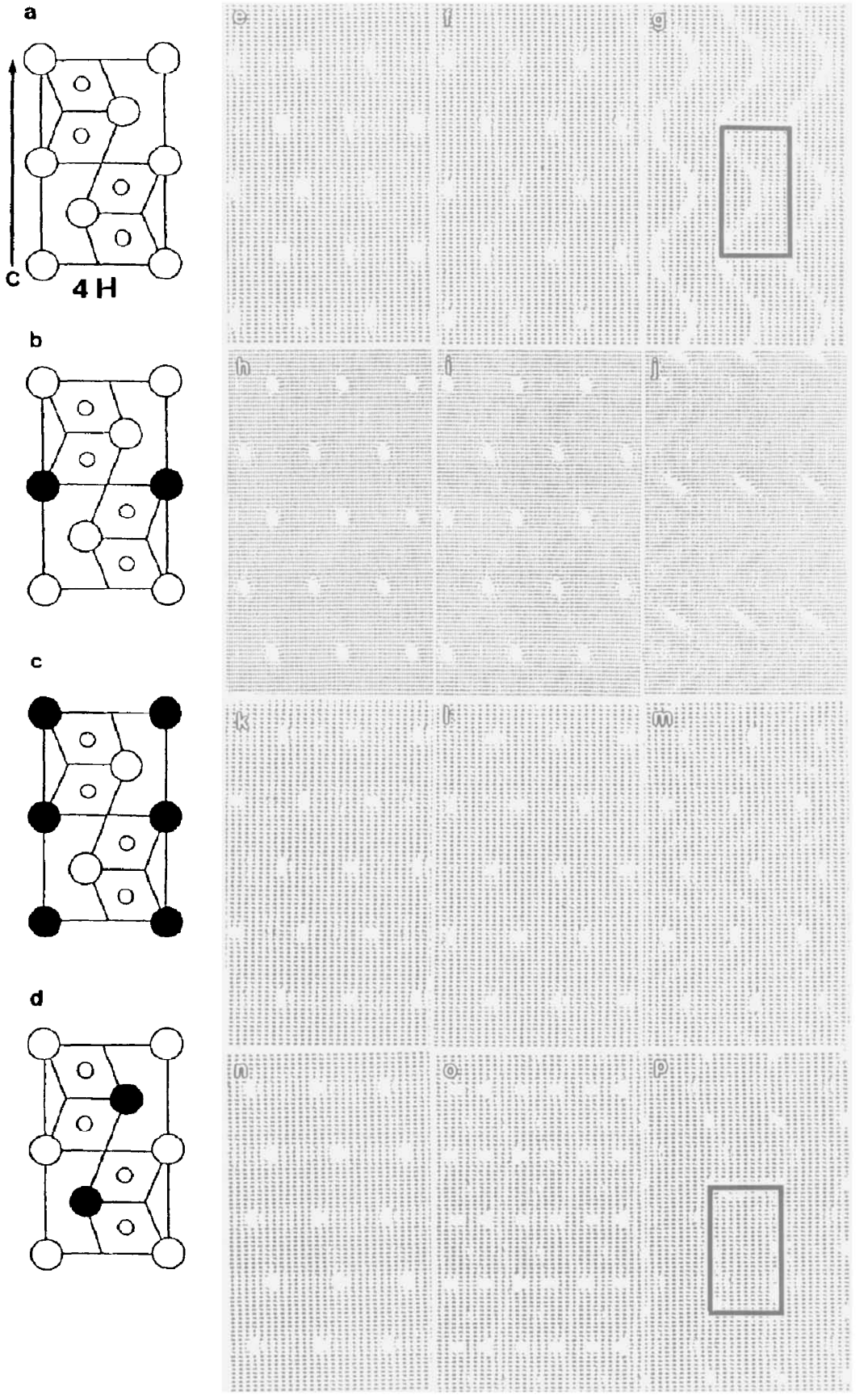
a
c
4 H
b
c
d

is seen in area B of Fig. 6a. The stacking faults seemed to be induced through introduction of Sr atoms. The formation of the stacking fault is clearly demonstrated by the corresponding electron diffraction pattern of Fig. 6b which shows the streaks in the diffraction spots along the c^*-axis in reciprocal space.

High-resolution electron microscope observations revealed the existence of an ordering due to the substituents for the samples prepared by heating sufficiently higher than 1150°C for 12 hr in O_2. Figures 9a and 9b show the high-resolution electron microscope image and electron diffraction pattern of the sample mixed with $SrCO_3$ of 0.15 mole ratio to $BaMnO_3$, respectively, which were taken with the incident electron beam parallel to the 010 direction in the hexagonal lattice. In this case, in the electron diffraction pattern comparing with that of Fig. 6b, the diffraction spots of an ordered phase as indicated by an arrow as well as the streaks due to stacking faults could be detected. Indices in the diffraction pattern of Fig. 9b are described in terms of $BaMnO_3$ (2H). Groups of white dots, in contrast, with a periodicity of about 0.9 nm, which corresponds to (001) spacing of a four-layer hexagonal structure, could be observed in the image of Fig. 9a. For contrast, calculation was done using the multi-slice method; the atomic positions in $BaMnO_3$ structure were adopted with strontium ions occupying some barium ion positions. Some structure models for calculation are shown in Figs. 10a–10d, which differ only in the manner of substituting for Ba-site in the four-layer structure. All the present structure models, which are represented by the symbol chh where c denotes cubic stacking of XO_3 layers in XYO_3, have more decreasing hexagonal character than that of two-layer $BaMnO_3$. Figure 10a is a basic structure model of the four-layer hexagonal cell and consists of only BaO_3 and MnO_6 layers. The large white circle and small one represent the Ba atoms and Mn atoms, respectively. The large black circles in Figs. 10b–10d denote the atomic positions of substituted sites for Ba-site with some Sr ions. Image calculations were carried out under the following imaging conditions: sample thickness = 8.5 nm; Δf = 50, 70, and 130 nm in underfocus; Cs = 1.4 mm; Cc = 1.8 mm; beam divergence angle = 1×10^{-3} rad, and accelerating voltage = 200 kV. The unit cell size of the four-layer hexagonal cell is drawn with the framework in Figs. 10g and 10p. The fact that the contrast in calculated images varies greatly through Figs. 10e–10p results from the difference in the power of atomic scattering factors for Ba and Sr. Contrast in calculated image of Fig. 10o or 10p was comparatively in good agreement with that of the observed image of Fig. 9a. The corresponding structure model described in Fig. 10d has the atomic positions of Sr atoms substituted for Ba-site ($Z = \frac{1}{4}, \frac{3}{4}$). The existence of a four-layer structure could be verified from the periodicity detected in image contrast but the atomic position of substitutions with Ba-site could not be determined closely from the image contrast, because there is no sufficiently distinctive difference in image contrast due to the atomic positions of substituents to distinguish between Figs. 10h–10p.

The results are summarized as follows: cation substitution by Sr or Ca ions in $BaMnO_3$ system induced a phase transformation of 2H phase into other phases with a longer periodicity than that of 2H structure

FIG. 10. Structure models and the corresponding calculated images by the multi-slice method. In the structure models of a–d, large white circles and black circles mean Ba and Sr atoms, respectively. In oxygen octahedra small circles represent Mn atoms. Unit cell size is drawn with the framework in the calculated image.

in order to avoid the electrostatic repulsion between XO_3 layers (X = Sr or Ca ions). The XO_3 layers, including Sr or Ca ions located in the X-site, led to edge-shared YO_6 octahedra and thus to the possibility of longer metal–metal distances than that of face-shared YO_6 octahedra. In $BaMnO_3$ (2H), the Mn–Mn distances across the infinite chains of face-shared octahedra must be 0.24 nm. On the other hand, in the four-layer structure the distance between them is about 0.31 nm. At the present stage, the stability of phases including small amounts of Sr or Ca ions in $BaMnO_3$ and the precise atomic positions of substitutions cannot be discussed yet on the basis of electron microscopic study.

Acknowledgment

The author expresses deep gratitude to Mr. M. Hofmann for correcting the manuscript.

References

1. P. C. DONOHUE, L. KATZ, AND R. WARD, *Inorg. Chem.* **5**(3), 339 (1966).
2. J. M. LONGO AND J. A. KAFALAS, *Mater. Res. Bull.* **3,** 687 (1968).
3. Y. SYONO, S. AKIMOTO, AND K. KOHN, *J. Phys. Soc. Japan* **26,** 993 (1969).
4. T. NEGAS AND R. S. ROTH, *J. Solid State Chem.* **3,** 323(1971).
5. B. L. CHAMBERLAND, A. W. SLEIGHT, AND J. F. WEIHER, *J. Solid State Chem.* **1,** 506 (1970).
6. A. HARDY, *Acta Crystallogr. Sect. B* **15,** 179 (1962).
7. H. SHIBAHARA AND H. HASHIMOTO, *in* "Proceedings, 7th International Conference on Crystal Growth, Stuttgart," *J. Cryst. Growth* **65,** 683 (1983).
8. H. SHIBAHARA, *J. Solid State Chem.* **66,** 116 (1987).
9. R. D. SHANNON AND C. T. PREWITT, *Acta Crystallogr. Sect. B* **25,** 925 (1969).
10. R. H. DUNGAN, D. H. KANE, AND L. R. BICKFORD, JR., *J. Amer. Ceram. Soc.* **35,** 318 (1952).
11. M. MCQUARRIE AND B. MALCOLM, *J. Amer. Ceram. Soc.* **38,** 447 (1955).
12. R. C. DEVRIES AND R. ROY, *J. Amer. Ceram. Soc.* **38,** 142 (1955).
13. J. M. COWELY AND A. F. MOODIE, *Acta Crystallogr.* **10,** 609 (1957).
14. P. GOODMAN AND A. F. MOODIE, *Acta Crystallogr. Sect. A* **30,** 280 (1974).